Am J Transl Res 2026;18(8):7034-7052
www.ajtr.org /ISSN:1943-8141/AJTR0172997

Original Article

FBXO11 and FBXO32 are associated with TRAF3-TBK1-IRF3 signaling components in chronic hepatitis B: evidence from clinical samples and preliminary mechanistic studies

Liqiang Li[1,2], Shun Tao[1,2], Yunfei Zhang[1,2], Zihan Zeng[1,2], Liang Li[1,2], Jun Zhang[1,2]

[1]Department of General Surgery, The Second People's Hospital of Hefei, Hefei Hospital Affiliated to Anhui Medical University, Hefei 230000, Anhui, China; [2]Department of General Surgery, Second People's Hospital Affiliated to Bengbu Medical University, Bengbu 233000, Anhui, China

Received March 30, 2026; Accepted June 30, 2026; Epub August 15, 2026; Published August 30, 2026

Abstract: Background: Chronic hepatitis B (CHB) remains a major global health burden despite the availability of effective vaccines and antiviral therapies. F-box proteins have been implicated in diverse biological processes, including immune regulation, but the potential involvement of FBXO11 and FBXO32 in host responses to HBV infection remains poorly understood. Aim: To investigate the expression patterns of FBXO11 and FBXO32 in CHB patients and explore their potential associations with components of the TRAF3-TBK1-IRF3 signaling pathway. Methods: We examined the expression levels of FBXO11 and FBXO32 in PBMCs derived from 30 CHB patients and controls. Protein-protein interactions were evaluated using co-immunoprecipitation and immunofluorescence assays in HEK293T cells. The effects of neddylation inhibition on protein expression and complex formation were examined using MLN4921 treatment. CRISPR/Cas9-mediated gene disruption and adeno-associated virus-mediated overexpression approaches were used for exploratory mechanistic studies. An HBV hydrodynamic injection mouse model was utilized to assess in vivo expression patterns. Results: FBXO11 and FBXO32 expression levels were significantly elevated in PBMCs from CHB patients compared with healthy controls and were accompanied by increased expression of TRAF3-TBK1-IRF3 pathway-related molecules. Co-immunoprecipitation analyses demonstrated associations of FBXO11 and FBXO32 with TRAF3, TBK1, and IRF3 in both clinical samples and HEK293T cells. Reciprocal enhancement of FBXO11 and FBXO32 expression was observed under overexpression conditions. Inhibition of neddylation reduced FBXO11 and FBXO32 protein abundance and weakened their associations with TRAF3-TBK1-IRF3 pathway components. In vivo experiments showed that HBV exposure was accompanied by increased hepatic expression of FBXO11 and FBXO32, and that genetic manipulation effectively altered their expression levels. Conclusion: FBXO11 and FBXO32 are upregulated in CHB and exhibit associations with components of the TRAF3-TBK1-IRF3 signaling network. These findings provide preliminary evidence supporting potential involvement of FBXO11 and FBXO32 in host immune-related signaling during HBV infection and warrant further investigation in physiologically relevant HBV infection models.

Keywords: FBXO11, FBXO32, hepatitis B virus, innate immunity, TRAF3-TBK1-IRF3 pathway, neddylation

Introduction

Hepatitis B virus (HBV) infection is a serious public health problem [1]. According to statistics, there were 7.3 million cases of HBV and 283.64 million cases of HBV-related liver cirrhosis in 2021 [2]. The hepatitis B vaccine is already in use, and as a result, the number of new infections has declined significantly. However, a functional cure remains elusive [3, 4]. Consequently, it is clinically important to explain the molecular mechanisms of HBV-host interactions and develop new therapeutic strategies.

The innate immune system is the body's first line of defense against any viral infection [5, 6]. When viruses enter host cells, the pattern recognition receptors (PRRs) detect viral nucleic acids present in the cell. Subsequently, these

https://doi.org/10.62347/SCRE1263

molecules generate type I interferons (IFNs) and pro-inflammatory cytokines [7]. The TBK1 (TANK-binding kinase 1) and IRF3 (Interferon regulatory factor 3) signaling pathway is crucial for the production of type I interferon [8, 9]. TRAF3 is necessary for the translocation of IRF3 from the cytoplasm to the nucleus upon viral infection. Essentially, this is a result of the phosphorylation of IRF3 by TRAF3-activated TBK1 [10, 11]. Regulation of innate immune signaling pathways through ubiquitination and neddylation is critical for their function and activity [12, 13]. F-box proteins are substrate recognition subunits of the SKP1-Cullin1-F-box (SCF) E3 ubiquitin ligase complex [14]. By recognizing specific substrates and mediating their ubiquitin-dependent degradation, F-box proteins regulate diverse cellular processes, including cell cycle, signal transduction, and transcription [15]. FBXO11 (F-box protein 11) and FBXO32 (F-box protein 32) represent important members of the F-box protein family. FBXO11 has been reported to be involved in regulating the TGF-β signaling pathway, the NF-κB signaling pathway, and the cell cycle process [16]. FBXO32 is a key regulatory factor for muscle atrophy, and it also participates in regulating cellular metabolism and immune responses [17]. In recent years, accumulating evidence has demonstrated that F-box protein family members play important roles in antiviral immunity. Overexpression of FBXO3 can inhibit the antiviral response of cells [18]. FBXO17 has been reported to negatively regulate the IFN-I signaling pathway triggered by double-stranded DNA, RNA or viral infections [19]. However, the functions of FBXO11 and FBXO32 in antiviral immunity have not been previously reported.

Considering this background, we hypothesized that FBXO11 and FBXO32 might play a role in host anti-HBV immune responses through modulation of the TRAF3-TBK1-IRF3 signaling pathway. Our investigations using clinical samples, exploratory cellular experiments, and animal studies provide preliminary observations regarding the expression patterns of FBXO11 and FBXO32 and their potential associations with TRAF3-TBK1-IRF3 signaling components in the context of HBV infection. Our results provide new avenues for studying F-box proteins in antiviral immunity and reveal possible targets for treatment of chronic hepatitis B.

Materials and methods

Clinical sample collection

Peripheral blood samples were collected from 30 patients with chronic hepatitis B (CHB) and 30 healthy controls at the Second People's Hospital of Hefei between January 2024 and December 2024. All patients had CHB according to the Guideline for Prevention and Treatment of CHB [20], were HBsAg positive for more than 6 months and had HBV DNA larger than 10^4 copies/mL. Peripheral blood mononuclear cells (PBMCs) can reflect systemic immunological activation resulting from HBV infection. This does not mean PBMCs have to be infected with HBV. Individuals were excluded with hepatitis C virus infection (HCV), hepatitis D virus infection (HDV) or human immunodeficiency virus infection, with autoimmune liver disease, with alcohol-related liver disease, with drug induced liver disease, and with other serious systematic diseases. Control subjects, who were HBsAg-negative and had normal liver function, were recruited from those undergoing routine physical examinations during the study period. The ethical committee of The Second People's Hospital of Hefei (Approval Number: 2023-Keyan-102) approved the protocol for this study. In addition, all participants provided written informed consent. Fasting peripheral blood (10 mL) was collected from each participant, and PBMCs were isolated using Ficoll gradient. The total RNA extraction was performed for a portion of the PBMCs. The rest of the cell pellets were stored at -80°C for protein extraction.

Sample size and statistical power considerations

This study employed a convenience sample of 30 CHB patients and 30 healthy controls matched for age and sex distribution. No formal a priori power calculation was conducted because (I) this was a single-center exploratory study with limited funding and recruitment timeframe; (II) no published data existed regarding the expected effect size for FBXO11/FBXO32 expression differences between CHB patients and healthy controls at the time of study design; and (III) the primary objective was hypothesis generation rather than definitive effect estimation. Post-hoc power analysis indi-

cated that with the observed effect sizes (Cohen's d ≈ 1.2-1.5 for mRNA and protein expression differences), the achieved power exceeded 0.80 for two-group comparisons at $\alpha = 0.05$; however, we recognize that post-hoc calculations are inherently biased and do not substitute for prospective power analysis. Future confirmatory studies should employ formal sample size calculations based on the effect sizes reported herein.

Cell culture and transfection

Human embryonic kidney 293T cells were obtained from the Cell Bank of the Chinese Academy of Sciences and cultured in DMEM medium (HyClone) supplemented with 10% fetal bovine serum (Gibco) and 1% penicillin-streptomycin (HyClone) at 37°C in a 5% CO_2 humidified incubator. 293T cells are a non-hepatic, non-immune transformed cell line, and there were used here only for preliminary mechanistic validation of protein-protein interactions, neddylation regulation, and mutual regulation, not for studying physiological HBV-specific antiviral innate immunity. The FBXO11 and FBXO32 overexpression plasmids pCMV-Myc-FBXO11 and pCMV-Myc-FBXO32 were constructed and maintained in our laboratory. Plasmid transfection was performed using Lipofectamine 3000 (Invitrogen) according to the manufacturer's instructions. Cells were collected 48 hours post-transfection for subsequent experiments. The CRISPR/Cas9 gene editing system was used to knockout FBXO11 and FBXO32 genes. The sgRNA sequences targeting FBXO11 and FBXO32 were designed using the CRISPR design tool (crispr.mit.edu). The sequences are available upon request. All sgRNAs were cloned into the lentiCRISPR v2 vector, and their targeting efficiency was validated by T7E1 assay and Sanger sequencing before use. The sgRNAs were cloned into the lentiCRISPR v2 vector, and lentiviruses were packaged and used to infect 293T cells. Stable knockout cell lines were obtained by selection with 2 μg/mL puromycin.

RT-qPCR analysis

Total RNA was extracted from cells or tissues using TRIzol reagent (Invitrogen) according to the manufacturer's protocol. Reverse transcription was performed using PrimeScript RT Master Mix (TaKaRa) to synthesize cDNA. Quantitative PCR was conducted using SYBR Premix Ex Taq II (TaKaRa) on an ABI 7500 Real-Time PCR System. The primer sequences for FBXO11, FBXO32, and GAPDH are available upon request. All primers were validated for specificity by melt curve analysis and agarose gel electrophoresis prior to use. GAPDH was used as the internal control, and the relative expression of target genes was calculated using the $2^{-\Delta\Delta Ct}$ method.

Western blot analysis

Using RIPA lysis buffer containing 1% PMSF and phosphatase inhibitors, total protein was extracted from the cells or tissues. The BCA method was used to determine the protein concentrations. Equal volumes of protein liquid samples were separated on an SDS-PAGE gel. Then, Western Blot transfer was performed onto PVDF membranes according to the manufacturer's instructions. The membranes were blocked with 5% skim milk for one hour and then incubated with primary antibodies at 4°C overnight. The primary antibodies included: anti-FBXO11 (1:1000, Abcam), anti-FBXO32 (1:1000, Abcam), anti-TRAF3 (1:1000, Cell Signaling Technology), anti-TBK1 (1:1000, Cell Signaling Technology), anti-p-TBK1 (Ser-172, 1:500, Cell Signaling Technology), anti-IRF3 (1:1000, Cell Signaling Technology), anti-p-IRF3 (Ser396, 1:500, Cell Signaling Technology), and anti-GAPDH (1:5000, Proteintech). After washing, the membranes were incubated with HRP-conjugated secondary antibodies at room temperature for 1 hour. Protein bands were visualized using ECL chemiluminescence reagent, and images were captured using the ChemiDoc XRS+ imaging system (Bio-Rad). Quantitative analysis was performed using ImageJ software.

Co-immunoprecipitation assay

Cells were collected and lysed in IP lysis buffer containing protease inhibitors and phosphatase inhibitors on ice for 30 minutes. After centrifugation at 12,000 rpm for 15 minutes at 4°C, the supernatant was collected. A fraction of the supernatant was kept aside as Input control, and the rest of the supernatant was left overnight at 4°C under gentle rotation with primary antibodies (anti-FBXO11 or anti-FBXO32, 2 μg). On the following day, Protein A/G magnetic beads (Thermo Fisher) were

added and incubated at room temperature for 2 hours. After washing the beads five times with IP lysis buffer, we added 2×SDS loading buffer. After boiling at 95°C for 10 min, the samples were analyzed by western blot for interacting proteins.

Immunofluorescence staining

Cells were seeded on glass coverslips and cultured overnight. After fixation with 4% paraformaldehyde for 15 minutes and permeabilization with 0.1% Triton X-100 for 10 minutes, cells were blocked with 5% BSA for 30 minutes. The cells were then incubated with anti-Myc antibody (1:500, Cell Signaling Technology) at 4°C overnight. The following day, Alexa Fluor 488-conjugated secondary antibody (1:1000, Invitrogen) was added and incubated at room temperature in the dark for 1 hour, followed by DAPI nuclear staining for 5 minutes. After mounting with anti-fade mounting medium, images were captured using a confocal microscope (Zeiss LSM 880).

Animal experiments

Female C57BL/6 mice (6-8 weeks old, weighing 18-22 g) were purchased from Beijing Vital River Laboratory Animal Technology Co., Ltd. and housed in a specific pathogen-free (SPF) facility. A total of 150 mice were randomly divided into 10 groups (15 mice per group): normal control group, HBV infection model group, FBXO11 overexpression + HBV group, FBXO32 overexpression + HBV group, FBXO11 knockout + HBV group, FBXO32 knockout + HBV group, and corresponding control groups. The HBV infection model was established by hydrodynamic injection of pAAV-HBV1.2 plasmid (10 μg per mouse) via tail vein [14]. Overexpression and knockout of FBXO11/FBXO32 were achieved by tail vein injection of corresponding adeno-associated viruses (AAV8 vector, 1×10^{11} vg per mouse) two weeks before HBV infection. Serum and liver tissue samples were collected at 0, 6, 12, 24, and 48 hours after HBV infection. These early time points were chosen to capture rapid innate immune signaling events and immediate early gene expression triggered by HBV introduction, rather than to model established, persistent HBV infection, which typically requires days to weeks after hydrodynamic injection. At each indicated time point, mice were deeply anesthetized by intraperitoneal injection of 10% chloral hydrate (400 mg/kg body weight) and then euthanized by cervical dislocation. Complete cessation of breathing and heartbeat was confirmed before tissue collection. Serum HBV DNA levels were detected by real-time quantitative PCR. Liver tissues were used for RT-qPCR, Western blot, HE staining, and immunohistochemistry analysis. All animal experiments described in this study were reviewed and approved by the Institutional Animal Care and Use Committee of Anhui Medical University.

Statistical analysis

All experiments were independently repeated at least three times. Quantitative data are presented as mean ± standard error of the mean (SEM). Comparisons between two groups were performed using independent sample t-test, and comparisons among multiple groups were performed using one-way ANOVA followed by Tukey's post hoc test. Statistical analysis was performed using SPSS 26.0 and GraphPad Prism 9.0 software. $P < 0.05$ was considered statistically significant.

Results

FBXO11 and FBXO32 are associated with TRAF3-TBK1-IRF3 pathway components in CHB

We first assessed the expression levels of FBXO11 and FBXO32 in PBMCs of CHB patients and healthy controls. PBMCs reflect the systemic immune status in CHB patients and do not represent direct HBV-infected target cells. We quantified the mRNA levels of FBXO11, FBXO32, TRAF3, TBK1 and IRF3 by RT-PCR and found that the mRNA levels of FBXO11, FBXO32, TRAF3, TBK1 and IRF3 were significantly higher in CHB patients than in healthy controls (**Figure 1**). Western blot further demonstrated increased protein levels of FBXO11, FBXO32, TRAF3, p-TBK1 and p-IRF3 in CHB patients, while the protein levels of total TBK1 and IRF3 were similar between the two groups (**Figure 2**). These data suggest that FBXO11 and FBXO32 are up-regulated during HBV infection and activation of the TRAF3-TBK1-IRF3 pathway may be involved.

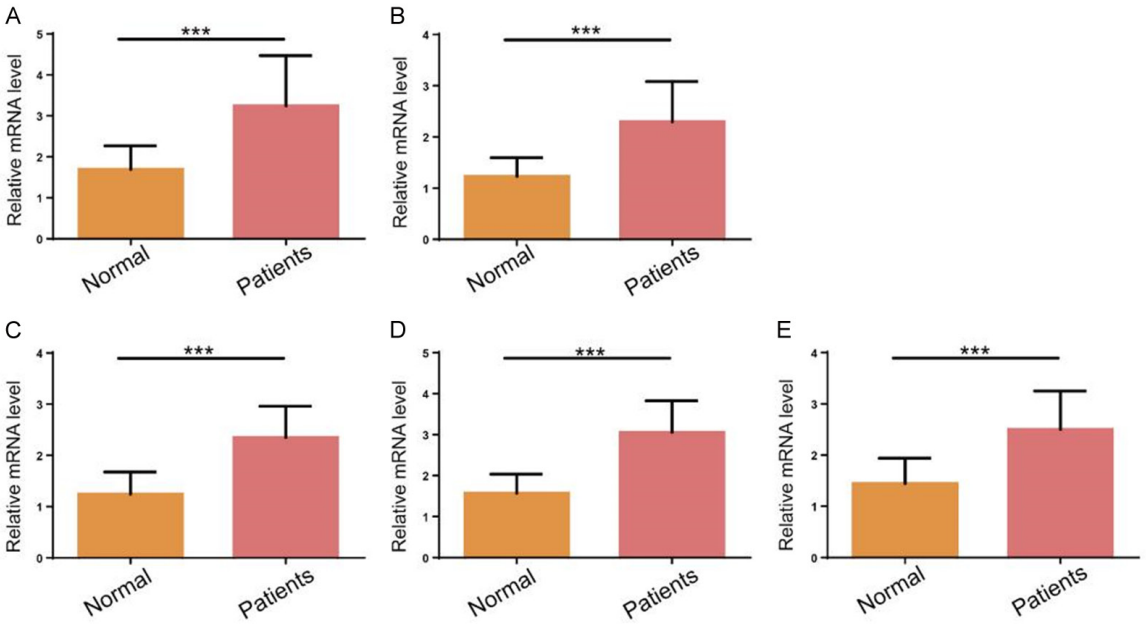

Figure 1. FBXO11 and FBXO32 are upregulated in CHB patients and are associated with expression of TRAF3-TBK1-IRF3 pathway components. (A, B) Relative mRNA levels of FBXO11 (A) and FBXO32 (B) in PBMCs from healthy controls and CHB patients were determined by RT-qPCR. (C-E) Relative mRNA levels of TRAF3 (C), TBK1 (D), and IRF3 (E) in PBMCs from healthy controls and CHB patients. ***P < 0.001. Abbreviations: CHB, chronic hepatitis B; PBMCs, peripheral blood mononuclear cells; RT-qPCR, reverse transcription quantitative polymerase chain reaction.

To explore whether FBXO11 and FBXO32 physically interact with components of the TRAF3-TBK1-IRF3 pathway, we performed Co-IP assays using PBMC lysates. FBXO11 was precipitated with IRF3, TRAF3, and TBK1 from normal subjects and CHB patients. However, the interactions were much stronger with CHB patients (**Figure 3A-C**). The interactions of FBXO32 with IRF3, TRAF3 and TBK1 were also augmented in CHB patients (**Figure 3D-F**). Together, our data reveal that both FBXO11 and FBXO32 are upregulated by HBV infection and form complexes with TRAF3-TBK1-IRF3 signaling pathway components.

Reciprocal expression changes of FBXO11 and FBXO32 in HEK293T cells

To explore the relationship between FBXO11 and FBXO32 expression under overexpression conditions, Myc-tagged expression plasmids were constructed and transfected into 293T cells. Cells were divided into four groups: control (293T+pCMV-Myc), FBXO11 overexpression (293T+pCMV-Myc-FBXO11), FBXO32 overexpression (293T+pCMV-Myc-FBXO32), and co-overexpression (293T+pCMV-Myc-FBXO11+pCMV-Myc-FBXO32). RT-qPCR analysis showed that overexpression of FBXO11 was accompanied by increased FBXO32 mRNA expression, whereas overexpression of FBXO32 was associated with elevated FBXO11 mRNA levels (**Figure 4A**, **4B**). Furthermore, cells subjected to co-overexpression exhibited higher expression levels of both FBXO11 and FBXO32 than those observed in the corresponding single-overexpression groups. Western blot analysis revealed similar expression patterns at the protein level (**Figure 4C**, **4D**).

Immunofluorescence staining demonstrated low basal fluorescence signals for FBXO11 and FBXO32 in control cells, whereas fluorescence intensity increased in the respective overexpression groups. The highest fluorescence intensity was observed in cells co-transfected with FBXO11 and FBXO32 expression plasmids (**Figure 5**). Quantitative analysis of fluorescence intensity yielded findings consistent with the RT-qPCR and Western blot results. Collectively, these data indicate reciprocal expression changes between FBXO11 and FBXO32 under the experimental conditions

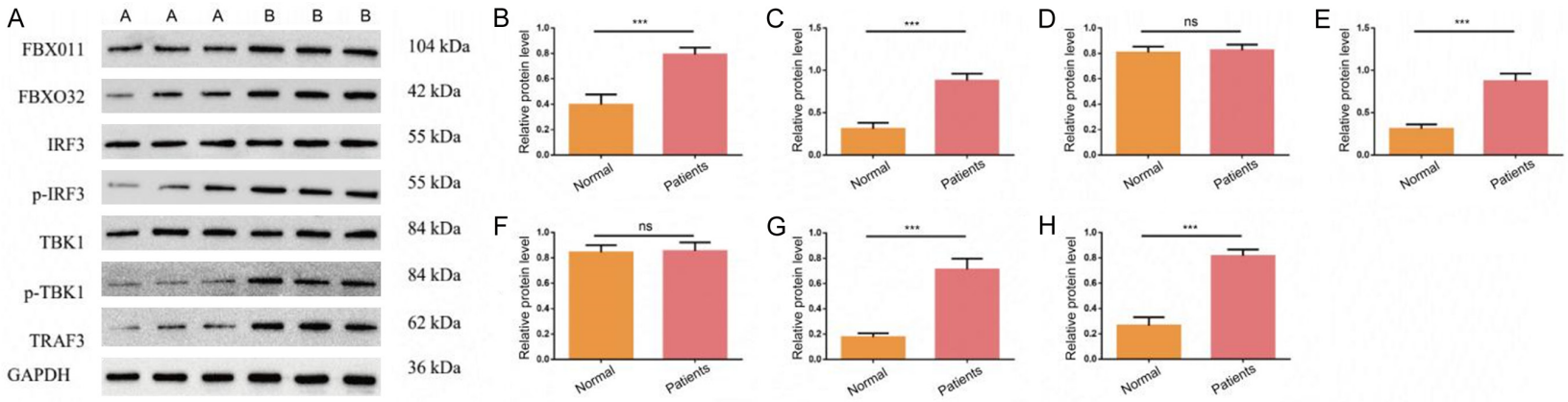

Figure 2. FBXO11 and FBXO32 protein levels and alterations in TRAF3-TBK1-IRF3 pathway-related proteins in CHB patients. (A) Representative Western blot images showing protein levels of FBXO11, FBXO32, IRF3, p-IRF3, TBK1, p-TBK1, TRAF3, and GAPDH in PBMCs from healthy controls (A) and CHB patients (B). (B-H) Quantitative analysis of FBXO11 (B), FBXO32 (C), IRF3 (D), p-IRF3 (E), TBK1 (F), p-TBK1 (G), and TRAF3 (H) protein levels. Ns, not significant; ***P < 0.001. Abbreviations: CHB, chronic hepatitis B; PBMCs, peripheral blood mononuclear cells; WB, Western blot; GAPDH, glyceraldehyde-3-phosphate dehydrogenase; p-, phosphorylated; ns, not significant.

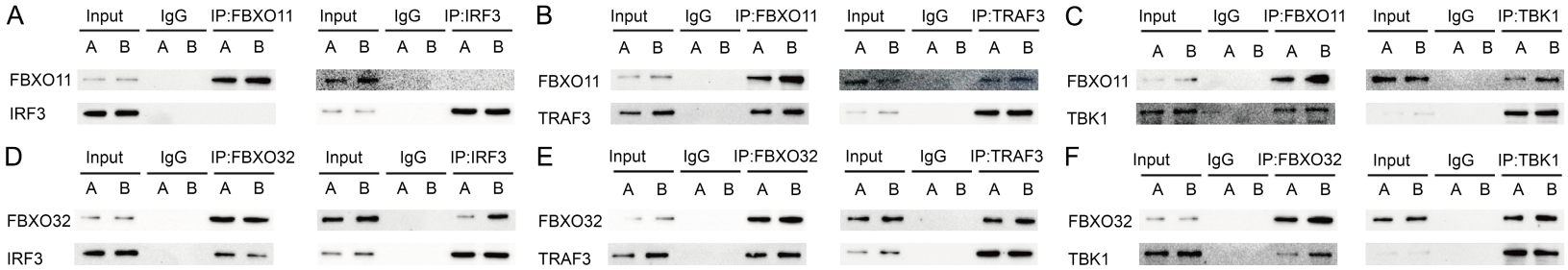

Figure 3. FBXO11 and FBXO32 interact with TRAF3-TBK1-IRF3 pathway components in CHB patients. Co-IP assays were performed using PBMC lysates from healthy controls (A) and CHB patients (B). (A) Interaction between FBXO11 and IRF3. (B) Interaction between FBXO11 and TRAF3. (C) Interaction between FBXO11 and TBK1. (D) Interaction between FBXO32 and IRF3. (E) Interaction between FBXO32 and TRAF3. (F) Interaction between FBXO32 and TBK1. Input indicates total cell lysates; IgG serves as negative control. Abbreviations: Co-IP, co-immunoprecipitation; PBMCs, peripheral blood mononuclear cells; CHB, chronic hepatitis B; Input, total cell lysates; IgG, immunoglobulin G (negative control).

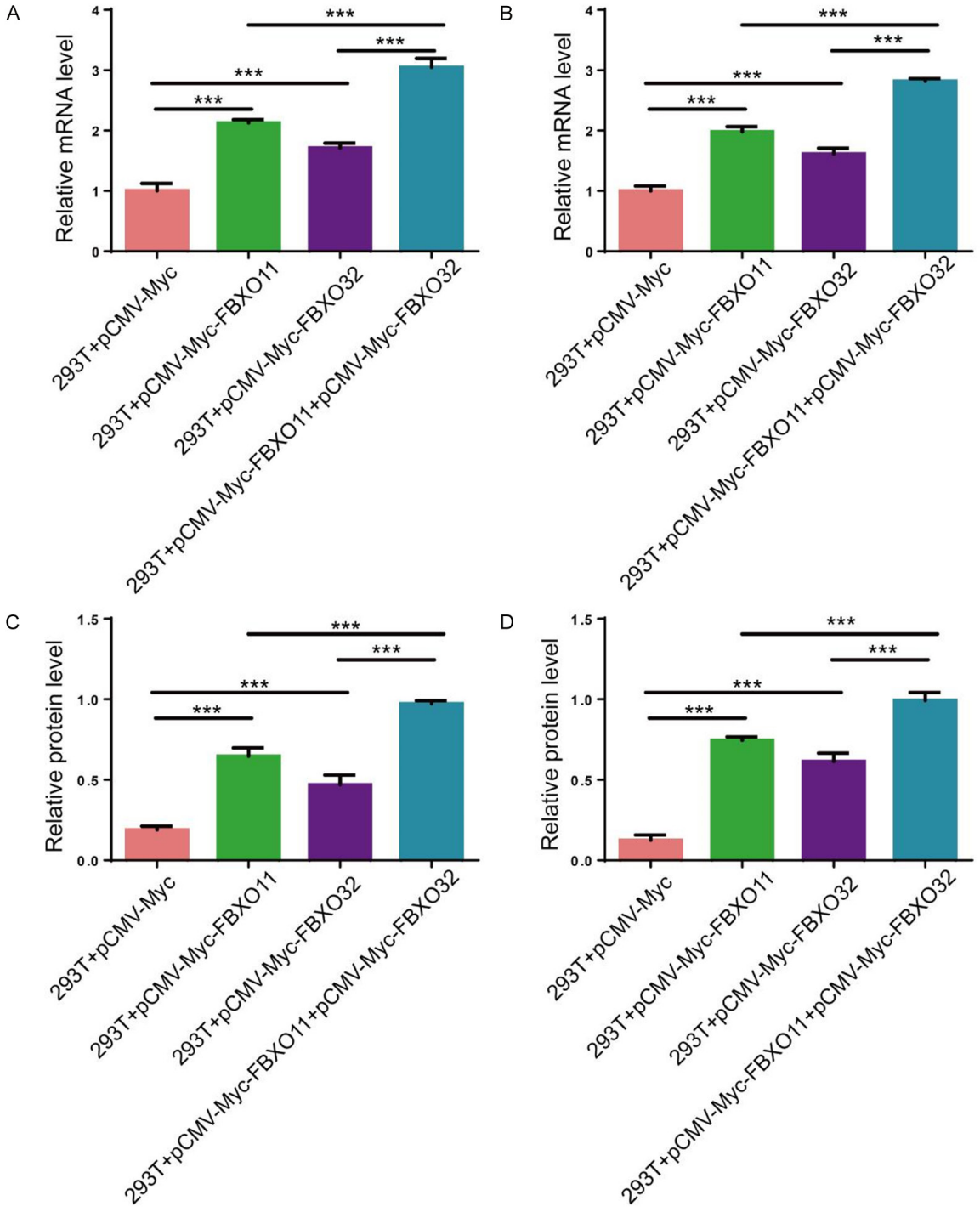

Figure 4. Reciprocal expression changes of FBXO11 and FBXO32 in overexpression experiments. (A, B) Relative mRNA levels of FBXO11 (A) and FBXO32 (B) in 293T cells transfected with control vector (pCMV-Myc), pCMV-Myc-FBXO11, pCMV-Myc-FBXO32, or both plasmids, as determined by RT-qPCR. (C, D) Relative protein levels of FBXO11 (C) and FBXO32 (D) in the same groups of cells, as determined by Western blot. ***P < 0.001. Abbreviations: RT-qPCR, reverse transcription quantitative polymerase chain reaction; WB, Western blot; pCMV-Myc, cytomegalovirus promoter-driven Myc-tagged expression vector.

employed. However, the present study did not investigate the molecular basis underlying these observations; therefore, no conclusions regarding feedback regulation, mutual stabilization, or direct mechanistic interactions can be drawn from the current data.

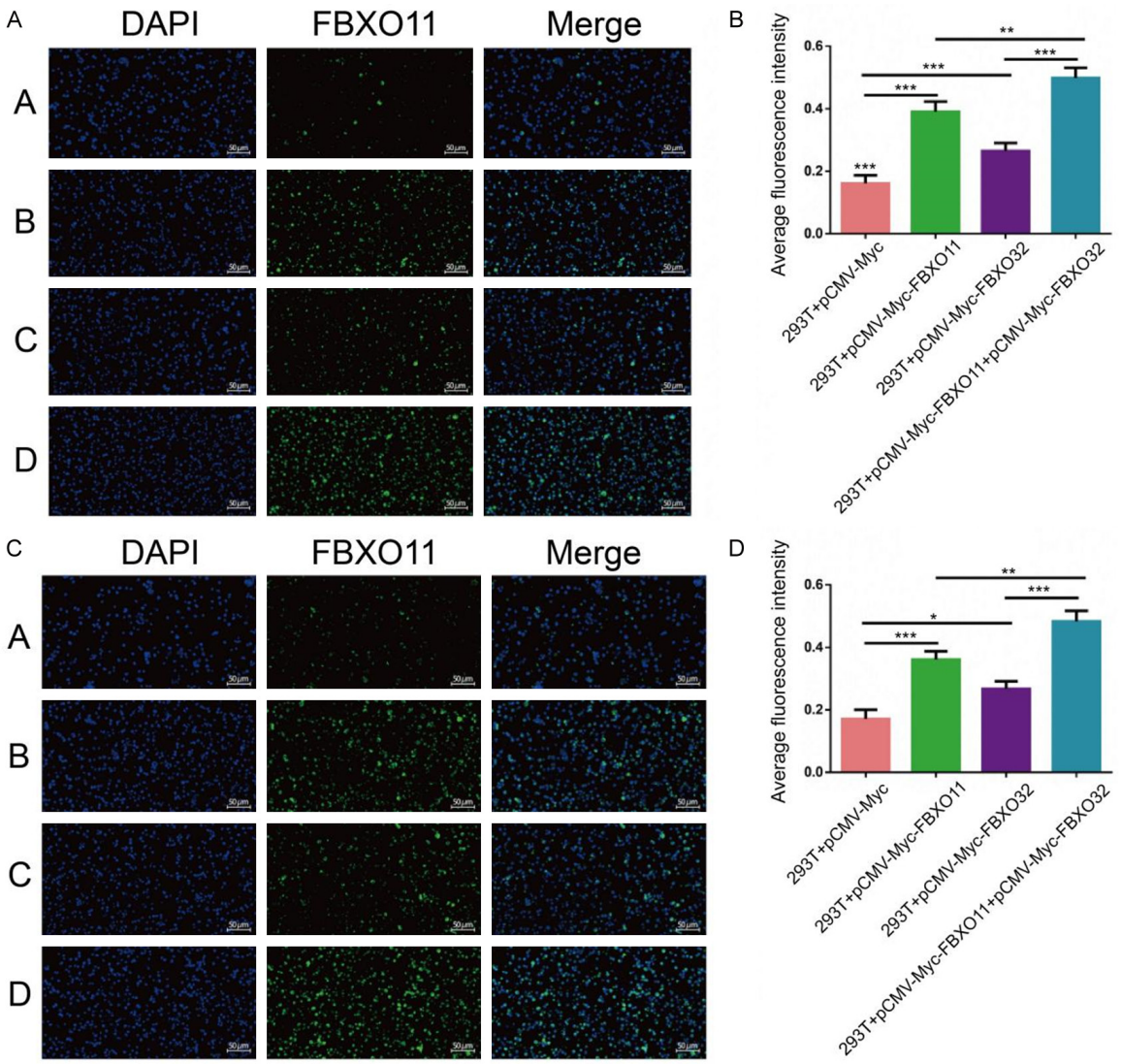

Figure 5. Immunofluorescence analysis of FBXO11 and FBXO32 expression under different overexpression conditions. A. Representative immunofluorescence images showing FBXO11 expression (green) and DAPI nuclear staining (blue) in 293T cells. Group A: control; Group B: FBXO11 overexpression; Group C: FBXO32 overexpression; Group D: FBXO11 and FBXO32 co-overexpression. Scale bar, 50 μm. B. Quantitative analysis of FBXO11 fluorescence intensity. C. Representative immunofluorescence images showing FBXO32 expression. D. Quantitative analysis of FBXO32 fluorescence intensity. *P < 0.05, **P < 0.01, ***P < 0.001. Abbreviations: IF, immunofluorescence; DAPI, 4',6-diamidino-2-phenylindole (nuclear counterstain).

Association of FBXO11 and FBXO32 with TRAF3-TBK1-IRF3 pathway proteins

To validate the interactions between FBXO11/FBXO32 and TRAF3-TBK1-IRF3 pathway components observed in clinical samples, we performed Co-IP assays in 293T overexpression cells. FBXO11 co-precipitated with IRF3, TRAF3, and TBK1, and these interactions were enhanced in cells overexpressing FBXO11 (**Figure 6A-C**). Reciprocal Co-IP using antibodies against IRF3, TRAF3, or TBK1 confirmed these interactions.

Similarly, FBXO32 was found to interact with IRF3, TRAF3, and TBK1 in overexpression cells (**Figure 6D-F**). Reciprocal Co-IP assays further validated these interactions. Notably, when both FBXO11 and FBXO32 were co-expressed, the interactions between each F-box protein and the pathway components were further enhanced, consistent with the reciprocal

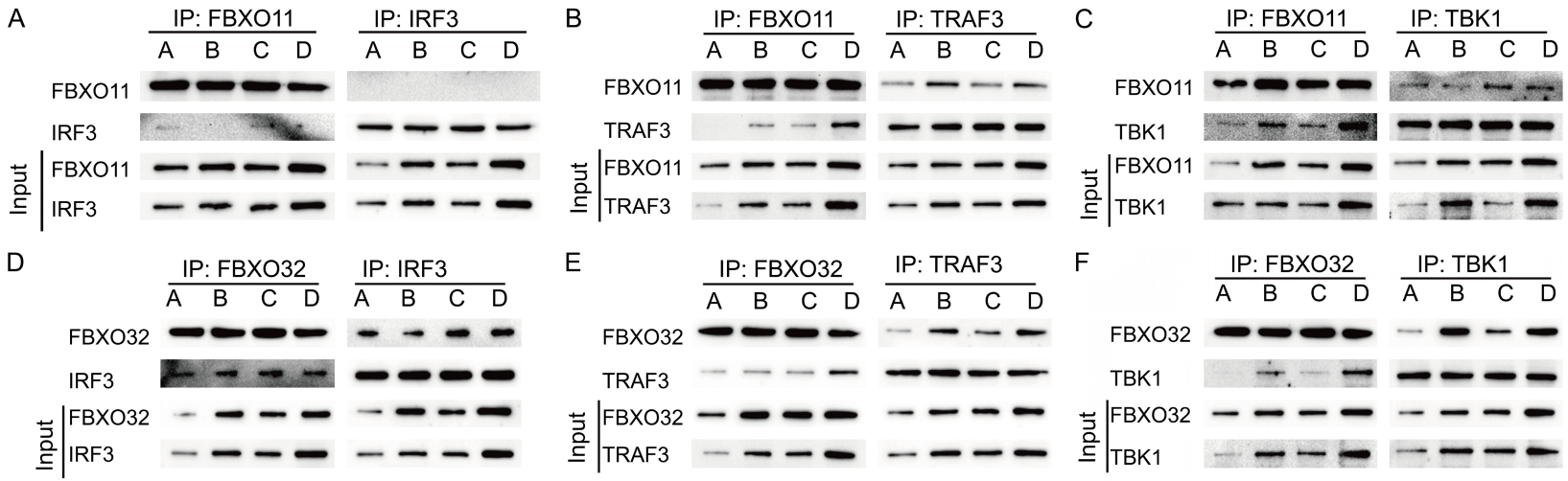

Figure 6. FBXO11 and FBXO32 interact with TRAF3-TBK1-IRF3 pathway components in overexpression cells. Co-IP assays were performed using 293T cell lysates. Groups: A, control; B, FBXO11 overexpression; C, FBXO32 overexpression; D, FBXO11 and FBXO32 co-overexpression. (A-C) FBXO11 interactions with IRF3 (A), TRAF3 (B), and TBK1 (C). (D-F) FBXO32 interactions with IRF3 (D), TRAF3 (E), and TBK1 (F). Abbreviations: Co-IP, co-immunoprecipitation; 293T, human embryonic kidney 293T cells.

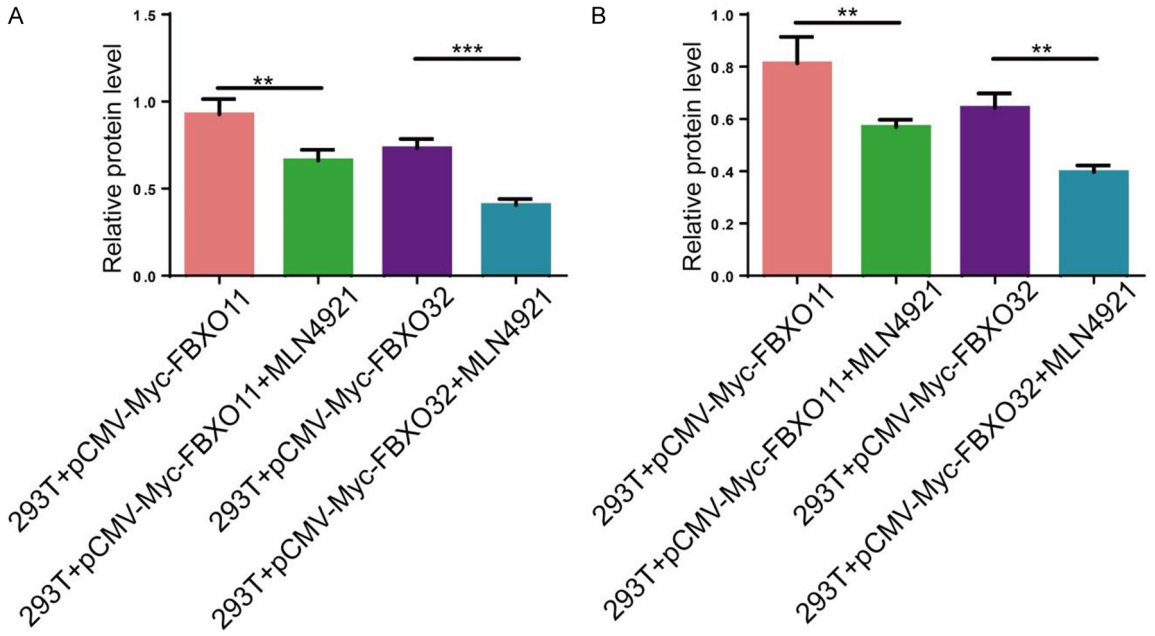

Figure 7. Neddylation inhibition reduces FBXO11 and FBXO32 protein abundance. (A, B) Relative protein levels of FBXO11 (A) and FBXO32 (B) in 293T cells treated with or without MLN4921 (NEDD8-activating enzyme inhibitor), as determined by Western blot. Group A: FBXO11 overexpression; Group B: FBXO11 overexpression + MLN4921; Group C: FBXO32 overexpression; Group D: FBXO32 overexpression + MLN4921. **P < 0.01, ***P < 0.001. Abbreviations: WB, Western blot; MLN4921, NEDD8-activating enzyme inhibitor.

expression changes observed under the same conditions. These results confirm that FBXO11 and FBXO32 physically associate with the TRAF3-TBK1-IRF3 signaling complex.

Neddylation inhibition influences FBXO11/FBXO32 protein abundance and protein associations

Given that F-box protein stability is regulated by neddylation, we investigated the effects of NEDD8-activating enzyme inhibition on FBXO11 and FBXO32. 293T cells overexpressing FBXO11 or FBXO32 were treated with MLN4921, a specific inhibitor of NEDD8-activating enzyme.

Western blot analysis revealed that MLN4921 treatment significantly reduced the protein levels of both FBXO11 and FBXO32 (**Figure 7**), indicating that neddylation modification is essential for maintaining the stability of these F-box proteins. The reduction was more pronounced when both FBXO11 and FBXO32 were co-expressed and treated with MLN4921.

Co-IP assays showed that MLN4921 treatment markedly attenuated the interactions between FBXO11 and IRF3, TRAF3, and TBK1 (**Figure 8A-C**). Similarly, neddylation inhibition impaired FBXO32 interactions with these pathway components (**Figure 8D-F**). These results demonstrate that neddylation not only stabilizes FBXO11 and FBXO32 but also facilitates their assembly with the TRAF3-TBK1-IRF3 signaling complex.

Validation of CRISPR/Cas9-mediated disruption of FBXO11 and FBXO32

To further elucidate the functional roles of FBXO11 and FBXO32, we employed the CRISPR/Cas9 gene editing system to establish stable knockout cell lines. Specific sgRNAs targeting FBXO11 or FBXO32 were cloned into the lentiCRISPR v2 vector. RT-qPCR analysis confirmed efficient knockdown of FBXO11 and FBXO32 at the mRNA level (**Figure 9A**, **9B**). Western blot analysis validated successful protein knockout, with marked reduction in FBXO11 and FBXO32 protein levels in single knockout cells and more pronounced reduction in double knockout cells (**Figure 9C**, **9D**). These pooled knockout populations were used for subsequent co-immunoprecipitation experi-

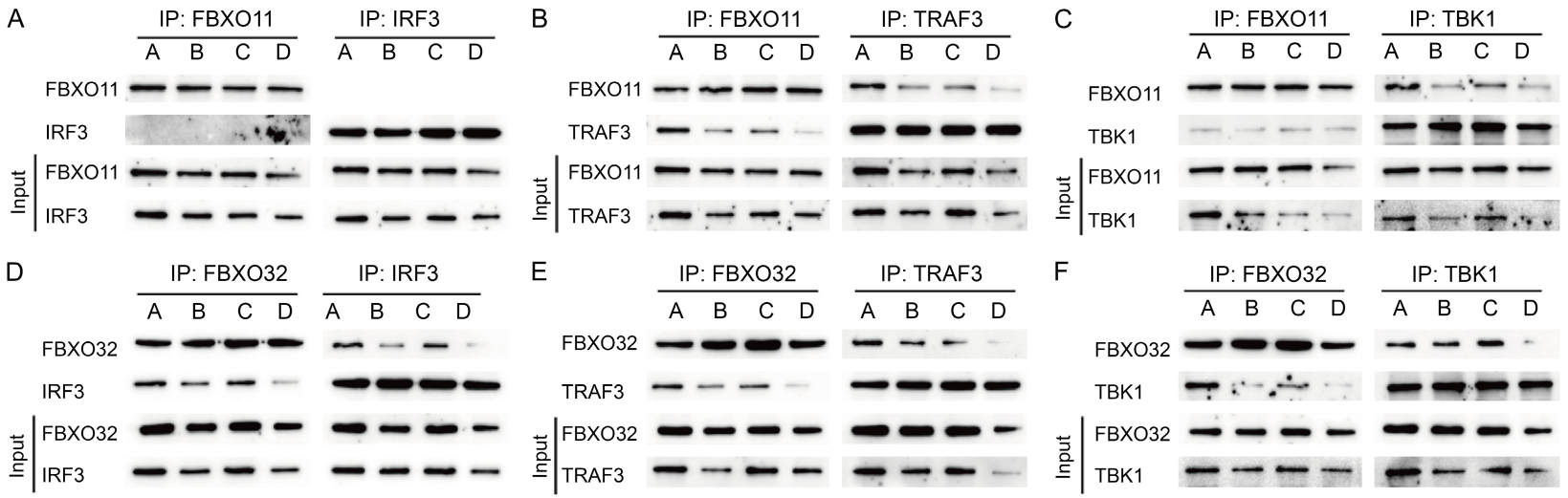

Figure 8. Neddylation inhibition influences the association of FBXO11 and FBXO32 with TRAF3-TBK1-IRF3 pathway components. Co-IP assays were performed using 293T cell lysates with or without MLN4921 treatment. Groups: A, FBXO11 overexpression; B, FBXO11 overexpression + MLN4921; C, FBXO32 overexpression; D, FBXO32 overexpression + MLN4921. (A-C) Effects of neddylation inhibition on FBXO11 interactions with IRF3 (A), TRAF3 (B), and TBK1 (C). (D-F) Effects of neddylation inhibition on FBXO32 interactions with IRF3 (D), TRAF3 (E), and TBK1 (F). Abbreviations: Co-IP, co-immunoprecipitation; MLN4921, NEDD8-activating enzyme inhibitor.

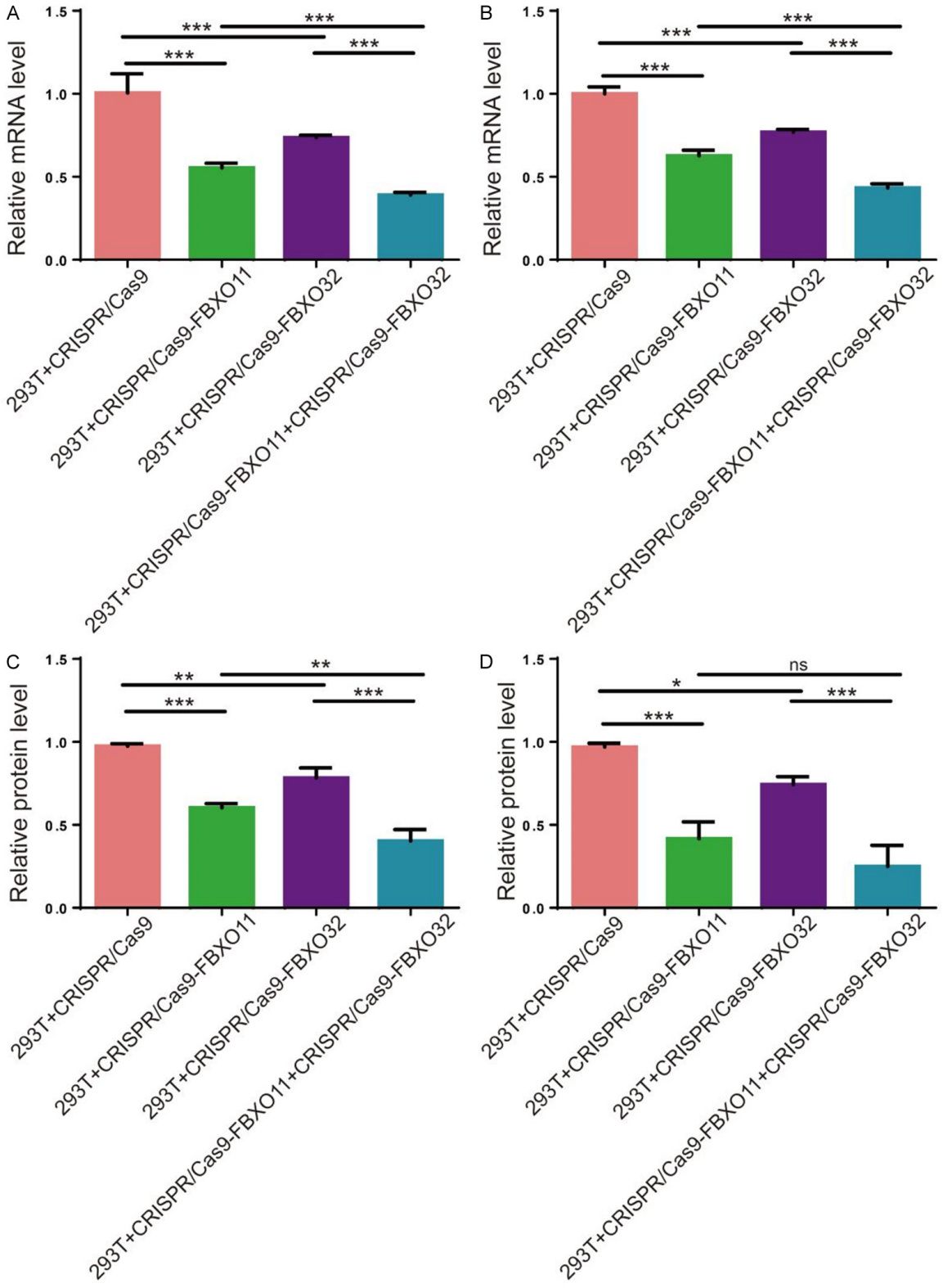

Figure 9. Validation of CRISPR/Cas9-mediated disruption of FBXO11 and FBXO32. (A, B) Relative mRNA levels of FBXO11 (A) and FBXO32 (B) in 293T cells with CRISPR/Cas9-mediated knockout, as determined by RT-qPCR. (C, D) Relative protein levels of FBXO11 (C) and FBXO32 (D) in the same groups, as determined by Western blot. *P < 0.05, **P < 0.01, ***P < 0.001; ns, not significant. Abbreviations: RT-qPCR, reverse transcription quantitative polymerase chain reaction; CRISPR/Cas9, clustered regularly interspaced short palindromic repeats/CRISPR-associated protein 9; WB, Western blot.

ments (**Figure 10**) and in vivo studies (**Figure 11**). No single-cell cloning or Sanger sequencing was performed to validate the specific indels; therefore, the knockout cell lines are characterized at the protein level only. Co-IP assays in knockout cells showed that depletion of FBXO11 weakened its interactions with IRF3, TRAF3, and TBK1 (**Figure 10A-C**), and similarly, FBXO32 knockout impaired its interactions with these pathway components (**Figure 10D-F**). These cell lines were subsequently used for animal experiments.

HBV exposure is accompanied by increased hepatic FBXO11 and FBXO32 expression

To validate our findings in an animal model, we established an HBV infection mouse model by hydrodynamic injection of the pAAV-HBV1.2 plasmid. The mice were divided into ten groups: a normal control group, an HBV infection model group, groups with FBXO11 or FBXO32 overexpression either with or without HBV infection, and groups with FBXO11 or FBXO32 knockout either with or without HBV infection.

RT-qPCR analysis of liver tissues revealed that HBV infection significantly increased FBXO11 and FBXO32 mRNA levels compared with normal controls (**Figure 11A**, **11B**). AAV8-mediated delivery successfully achieved overexpression of FBXO11 or FBXO32, while CRISPR/Cas9-mediated knockout effectively reduced their expression. Notably, HBV infection further enhanced the expression of exogenous FBXO11 and FBXO32.

These results were also confirmed at the protein level by Western blot analysis (**Figure 11C**, **11D**). HBV infection led to elevated FBXO11 and FBXO32 protein levels, which were further increased upon overexpression and decreased upon knockout. Overall, these in vivo findings align with the clinical data and support a role for FBXO11 and FBXO32 in immediate early host innate immune responses to HBV introduction. These data only confirm that genetic manipulation and HBV challenge altered FBXO11 and FBXO32 expression, without assessing functional consequences on intrahepatic immune signaling, hepatic inflammation, or key virological outcomes including serum HBV DNA and liver HBsAg levels. It should be noted that the early time points (0-48 h) reflect rapid signaling events rather than established chronic HBV infection, which requires days to weeks to develop after hydrodynamic injection.

Discussion

The present study investigated the expression patterns of FBXO11 and FBXO32 in chronic hepatitis B (CHB) and explored their potential associations with components of the TRAF3-TBK1-IRF3 signaling pathway. Through analyses of clinical PBMC samples, exploratory cellular experiments, and in vivo studies, we observed that FBXO11 and FBXO32 were significantly upregulated in CHB patients and were accompanied by increased expression of several molecules involved in innate immune signaling. In addition, co-immunoprecipitation analyses suggested that FBXO11 and FBXO32 may associate with TRAF3, TBK1, and IRF3 under the experimental conditions employed. These observations provide preliminary evidence supporting a possible relationship between FBXO11/FBXO32 and immune-related signaling pathways in the setting of chronic HBV infection. Importantly, the current findings should be interpreted with caution. The present study primarily identifies expression changes and protein associations rather than demonstrating direct functional regulation of antiviral immunity. Therefore, our results should be considered hypothesis-generating and provide a framework for future mechanistic investigations.

F-box proteins have emerged as important regulators of innate immune responses, with distinct family members exhibiting either positive or negative regulatory functions [21, 22]. One notable observation was the reciprocal change of FBXO11 and FBXO32 expression in overexpression experiments. Increased expression of either protein was accompanied by elevated expression of the other, while simultaneous overexpression produced the greatest expression levels. These findings suggest a potential relationship between FBXO11 and FBXO32; however, the underlying mechanism remains unclear. Several possibilities may explain this observation. FBXO11 and FBXO32 may share common upstream regulatory factors, participate in related transcriptional programs, or indirectly influence each other's expression through intermediate signaling molecules.

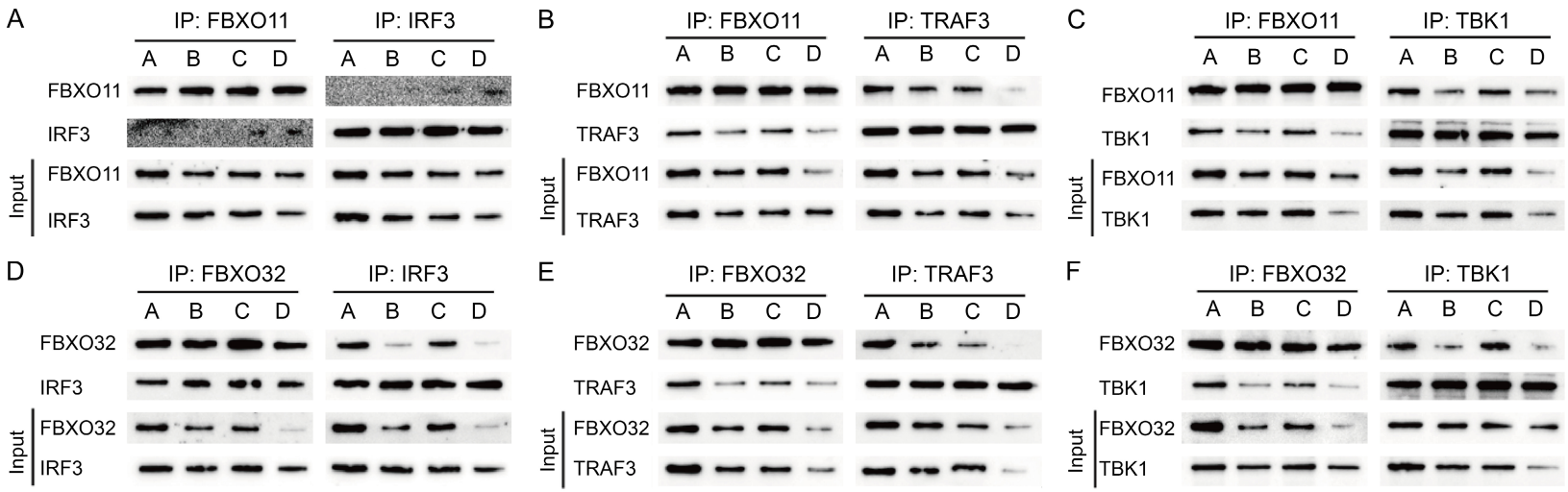

Figure 10. Effects of FBXO11 and FBXO32 disruption on associations with TRAF3-TBK1-IRF3 pathway components. Co-IP assays were performed using 293T cell lysates with CRISPR/Cas9-mediated knockout. Groups: A, control; B, FBXO11 knockout; C, FBXO32 knockout; D, FBXO11 and FBXO32 double knockout. (A-C) Effects of FBXO11 knockout on interactions with IRF3 (A), TRAF3 (B), and TBK1 (C). (D-F) Effects of FBXO32 knockout on interactions with IRF3 (D), TRAF3 (E), and TBK1 (F). Abbreviations: Co-IP, co-immunoprecipitation; CRISPR/Cas9, clustered regularly interspaced short palindromic repeats/CRISPR-associated protein 9.

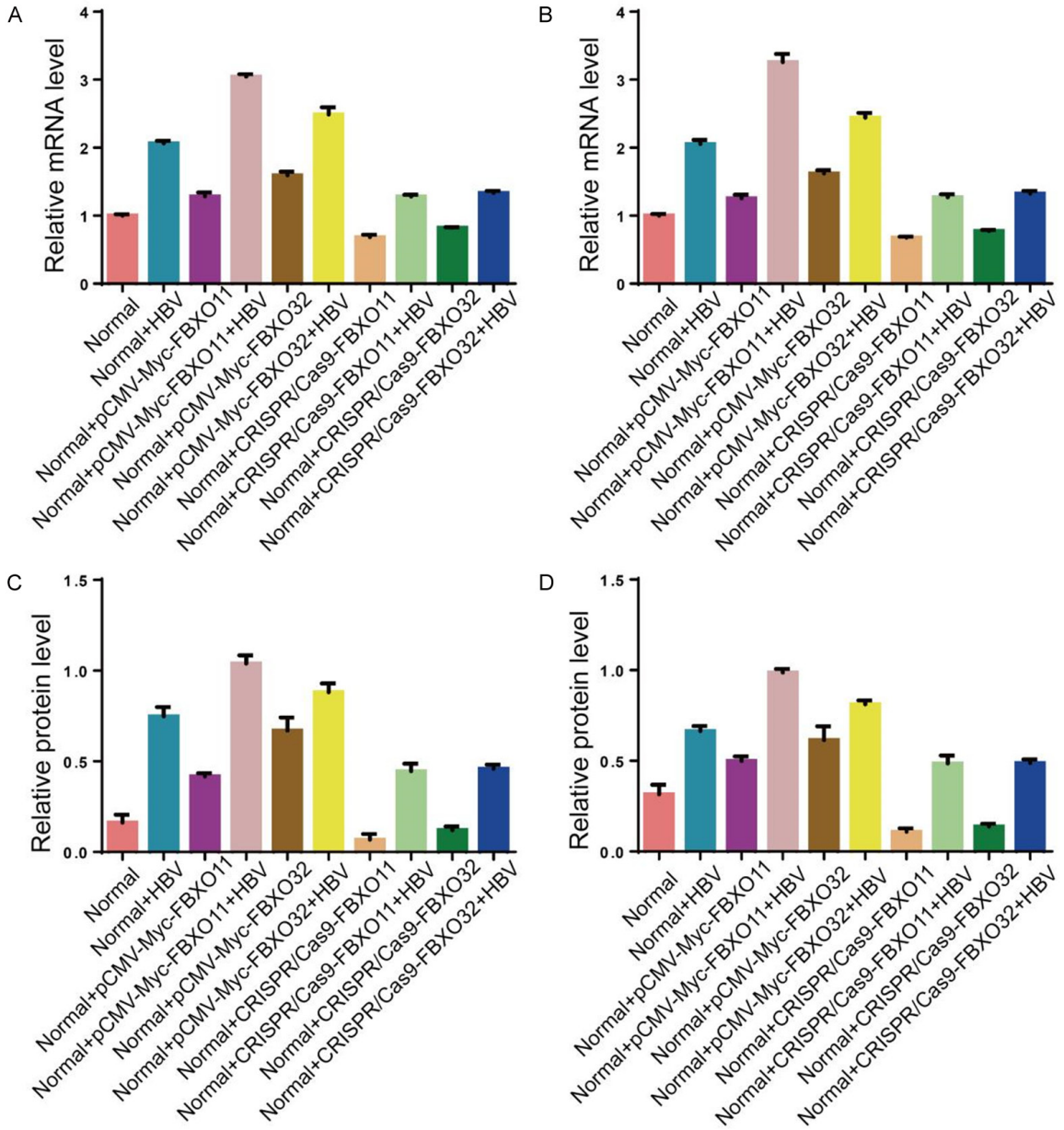

Figure 11. HBV exposure is accompanied by increased hepatic expression of FBXO11 and FBXO32. (A, B) Relative mRNA levels of FBXO11 (A) and FBXO32 (B) in mouse liver tissues from different experimental groups, as determined by RT-qPCR. (C, D) Relative protein levels of FBXO11 (C) and FBXO32 (D) in the same groups, as determined by Western blot. Groups: Normal, normal control; HBV, HBV infection model; +pCMV-Myc-FBXO11/32, overexpression; +CRISPR/Cas9-FBXO11/32, knockout. Abbreviations: RT-qPCR, reverse transcription quantitative polymerase chain reaction; WB, Western blot; HBV, hepatitis B virus; AAV8, adeno-associated virus serotype 8; CRISPR/Cas9, clustered regularly interspaced short palindromic repeats/CRISPR-associated protein 9.

Additionally, FBXO family members such as FBXO21 and FBXO43 have been shown to participate in complex regulatory networks that involve coordinated expression changes [23, 24]. Alternatively, the observed changes may reflect non-physiological effects associated with plasmid overexpression systems. Because mRNA stability assays, promoter activity analyses, protein turnover studies, and domain-mapping experiments were not performed, no conclusions regarding feedback regulation or mutual stabilization can be drawn from the cur-

rent data. Further mechanistic studies will be required to clarify the biological basis of this association.

The TRAF3-TBK1-IRF3 axis is a well-established signaling pathway involved in innate immune responses to viral infection [25, 26]. Another important observation in our study was the association of FBXO11 and FBXO32 with TRAF3, TBK1, and IRF3 detected by co-immunoprecipitation assays. Previous studies have reported that FBXO11 may participate in signaling events related to this pathway [10]. Our findings extend these observations by identifying FBXO32 as an additional protein that may be associated with components of the same signaling network. HTATSF1 has been shown to regulate innate antiviral immune responses by orchestrating TRAF3-IRF3 pathways [26], suggesting that multiple regulatory proteins converge on this signaling node. Nevertheless, co-immunoprecipitation data demonstrate protein association rather than functional activity. The present study did not evaluate TBK1 phosphorylation, IRF3 activation, type I interferon production, interferon-stimulated gene expression, or HBV replication. Importantly, the presence of physical interactions does not necessarily predict functional outcomes, as adaptor proteins can bind signaling components without activating them [11, 27]. Consequently, it remains unknown whether the observed protein associations result in meaningful functional effects on innate immune signaling. Future studies employing pathway activation assays and physiologically relevant HBV infection systems will be necessary to address these questions.

The present study also suggests a potential role for neddylation in maintaining FBXO11 and FBXO32 protein abundance and their associations with TRAF3-TBK1-IRF3 pathway components. Treatment with the NEDD8-activating enzyme inhibitor MLN4921 reduced FBXO11 and FBXO32 protein levels and weakened their detectable associations with signaling proteins. These findings are consistent with previous reports indicating that neddylation contributes to the regulation of protein stability and protein-protein interactions [12, 13]. Neddylation has been shown to influence diverse immune-related pathways, including inflammasome activation and viral lytic reactivation [28, 29]. Moreover, neddylation can modulate non-cullin substrates and affect signaling complex assembly in a context-dependent manner [30, 31]. However, the current data do not establish whether FBXO11 or FBXO32 are direct neddylation substrates, nor do they identify the specific molecular mechanisms involved. It remains possible that MLN4921 treatment exerts indirect effects on FBXO11/FBXO32 stability by inhibiting cullin-RING ligase activity, which regulates the turnover of upstream signaling molecules [30]. Additional biochemical studies will be required to determine whether neddylation directly modifies FBXO11 and FBXO32 or indirectly influences their stability through broader effects on cullin-RING ubiquitin ligase activity.

The in vivo experiments primarily served to evaluate expression patterns of FBXO11 and FBXO32 following HBV exposure and genetic manipulation. HBV hydrodynamic injection was associated with increased hepatic expression of both proteins, while AAV-mediated overexpression and CRISPR/Cas9-mediated disruption effectively altered their expression levels in liver tissues. However, these experiments did not assess downstream signaling activity, inflammatory responses, liver pathology, viral antigen expression, or HBV replication markers. FBXO2 and FBXO24 have been implicated in various pathological conditions through distinct mechanisms [32, 33], suggesting that F-box proteins exhibit diverse functional roles depending on cellular context. Therefore, the animal data should be interpreted as supportive expression-based observations rather than mechanistic validation of antiviral immune regulation. A predictive model based on the FBXO family has revealed the significance of cyclin F in hepatocellular carcinoma [34], indicating that FBXO family members may serve as useful biomarkers in liver diseases. Future studies incorporating virological and immunological endpoints will be necessary to determine the biological significance of FBXO11 and FBXO32 in HBV infection in vivo.

Several additional limitations warrant consideration. First, the clinical cohort was relatively small (30 CHB patients) and lacked stratification by disease phase. Second, PBMCs reflect systemic immune activation rather than intrahepatic events; we did not have access to

paired liver biopsy samples. Third, our CRISPR/Cas9 knockout cells were generated as pooled populations validated only by Western blot, without single-cell cloning or Sanger sequencing to confirm biallelic knockout. Fourth, the study did not evaluate type I interferon production or ISG expression, which are essential functional readouts of TBK1-IRF3 pathway activation. FBXO11 has been reported to promote ubiquitination of various substrates including β-catenin and Snail family transcription factors [35, 36], while FBXO32 can ubiquitinate PTEN and D-type cyclins [17, 37]. Whether FBXO11 and FBXO32 exert similar E3 ligase activities toward TRAF3 or TBK1 remains to be investigated. Furthermore, TBK1 itself is subject to multiple post-translational modifications including ubiquitination and acetylation [38, 39], and it is unknown whether FBXO11/FBXO32 influence these modifications. In summary, this study demonstrates that FBXO11 and FBXO32 are significantly upregulated in CHB and are associated with components of the TRAF3-TBK1-IRF3 signaling pathway. The present findings should be interpreted as preliminary and primarily associative. Further investigations using hepatocyte-based HBV infection systems and immune-competent models will be necessary to determine the physiological significance of these observations.

Conclusion

In summary, this study demonstrates that FBXO11 and FBXO32 are significantly upregulated in PBMCs from patients with chronic hepatitis B and are associated with components of the TRAF3-TBK1-IRF3 signaling pathway. We further observed physical associations between FBXO11/FBXO32 and TRAF3, TBK1, and IRF3 in exploratory cellular experiments, together with reciprocal enhancement of FBXO11 and FBXO32 expression under overexpression conditions. In addition, neddylation appeared to influence the stability of FBXO11 and FBXO32 and their associations with signaling complex components. Importantly, the present findings should be interpreted as preliminary and primarily associative. The study does not establish direct regulation of antiviral immunity, interferon production, or HBV replication by FBXO11 or FBXO32. Further investigations using hepatocyte-based HBV infection systems, primary human liver cells, and immune-competent models will be necessary to determine the physiological significance and functional consequences of these observations. Overall, our findings expand current knowledge regarding FBXO family proteins in the context of chronic hepatitis B and provide a basis for future mechanistic studies of FBXO11 and FBXO32 in HBV-associated host responses.

Acknowledgements

This work was supported by the Clinical Medicine Transformation Project of Anhui Province (No. 202304295107020093).

Disclosure of conflict of interest

None.

Address correspondence to: Jun Zhang, Department of General Surgery, The Second People's Hospital of Hefei, Hefei Hospital Affiliated to Anhui Medical University, No. 246, Heping Road, Yaohai District, Hefei 230000, Anhui, China. Tel: +86-0551-62965392; E-mail: doc_zhangjun@163.com

References

[1] GBD 2019 Hepatitis B Collaborators. Global, regional, and national burden of hepatitis B, 1990-2019: a systematic analysis for the Global Burden of Disease Study 2019. Lancet Gastroenterol Hepatol 2022; 7: 796-829.

[2] Danpanichkul P, Duangsonk K, Chen VL, Saokhieo P, Dejvajara D, Sukphutanan B, Aboona MB, Lopimpisuth C, Pang Y, Ibrahim AF, Fallon MB, Huang DQ, Kim D, Singal AG, Yang JD, Aqel BA, Terrault NA and Wijarnpreecha K. Global burden of HBV-related liver disease: Primary liver cancer due to chronic HBV infection increased in over one-third of countries globally from 2000 to 2021. Hepatology 2025; 82: 1274-1286.

[3] Yan Q, Fu X, Wang Y and Wang G. Do the therapeutic vaccines hold hope for the treatment of hepatitis B? Hepatol Int 2025; 19: 1320-1330.

[4] Papatheodoridi M and Papatheodoridis G. Nucleos(t)ide analogue treatment in hepatitis B: to stop or not to stop? Expert Rev Anti Infect Ther 2026; 24: 113-120.

[5] Warrick KA, Vallez CN, Meibers HE and Pasare C. Bidirectional communication between the innate and adaptive immune systems. Annu Rev Immunol 2025; 43: 489-514.

[6] Jin S, He X, Wang Z, Zhou T, Wang J, Pan G, Zhang Y, Ma L, Yang S, Wang L, Wu Y, Zou Y, Qi N and Cui J. Oxaloacetate sensing promotes innate immune antiviral defence against influenza virus infection. Nat Microbiol 2025; 10: 2521-2536.

[7] Asadi-Asadabad S, Sarvnaz H, Amiri MM, Mobini M, Khoshnoodi J, Hojjat-Farsangi M, Jeddi-Tehrani M, Golsaz-Shirazi F and Shokri F. Influence of pattern recognition receptor ligands on induction of innate immunity and control of hepatitis B virus infection. Viral Immunol 2021; 34: 531-541.

[8] Wang W, Zhi L, Liu S, Zhao Y, Zhang Y, Qin Q, Huang X and Huang Y. Singapore grouper iridovirus VP018 abrogates the interferon response by targeting STING-TBK1-IRF3 axis. Int J Biol Macromol 2025; 311: 144011.

[9] Liang Y, Liang Y, Wang Q, Li Q, Huang Y, Li R, Pan X, Lie L, Xu H, Han Z, Liu H, Wen Q, Zhou C, Ma L and Zhou X. Viperin inhibits interferon-γ production to promote Mycobacterium tuberculosis survival by disrupting TBK1-IKKε-IRF3-axis and JAK-STAT signaling. Inflamm Res 2024; 73: 897-913.

[10] Gao L, Gao Y, Han K, Wang Z, Meng F, Liu J, Zhao X, Shao Y, Shen J, Sun W, Liu Y, Xu H, Du X, Li J and Qin FX-F. FBXO11 amplifies type I interferon signaling to exert antiviral effects by facilitating the assemble of TRAF3-TBK1-IRF3 complex. J Med Virol 2023; 95: e28655.

[11] Zhang W, Weng J, Yao L, Jia P, Yi M and Jia K. Nectin4 antagonises type I interferon production by targeting TRAF3 for autophagic degradation and disrupting TRAF3-TBK1 complex formation. Int J Biol Macromol 2022; 218: 654-664.

[12] Zhu J, Chu F, Zhang M, Sun W and Zhou F. Association between neddylation and immune response. Front Cell Dev Biol 2022; 10: 890121.

[13] Zhang S, Yu Q, Li Z, Zhao Y and Sun Y. Protein neddylation and its role in health and diseases. Signal Transduct Target Ther 2024; 9: 85.

[14] Dai M, Chen S, Wang Y, Fan J, Pan X, Sang C, Liu Y, Hu M, Ma L and Wang S. F-box proteins at the crossroads of ubiquitination and tumor immunity: regulatory networks and immunotherapy strategies. Front Immunol 2025; 16: 1596344.

[15] Zheng N, Wang Z and Wei W. Ubiquitination-mediated degradation of cell cycle-related proteins by F-box proteins. Int J Biochem Cell Biol 2016; 73: 99-110.

[16] Xu J, Zhi X, Zhang Y and Ding R. Tanshinone IIA alleviates IL-1β-induced chondrocyte apoptosis and inflammation by regulating FBXO11 expression. Clinics (Sao Paulo) 2024; 79: 100365.

[17] Li F, Yu H, Zhang Y, Ma Y, Chen X, Zhang J, Sun L, Guo R, Wu Y, Zheng P, Wang X, Bie P, He F, Zhang L, Xie C and Xiong H. F-box protein FBXO32 ubiquitinates and stabilizes D-type cyclins to drive cancer progression. Nat Commun 2025; 16: 4060.

[18] Li Z, Fan S, Wang J, Chen X, Liao Q, Liu X, Ouyang G, Cao H and Xiao W. Zebrafish F-box protein fbxo3 negatively regulates antiviral response through Promoting K27-linked polyubiquitination of the transcription factors irf3 and irf7. J Immunol 2020; 205: 1897-1908.

[19] Peng D, Wang Z, Huang A, Zhao Y and Qin FX. A novel function of F-box protein FBXO17 in negative regulation of Type I IFN signaling by recruiting PP2A for IFN regulatory factor 3 deactivation. J Immunol 2017; 198: 808-819.

[20] Xie Yandi, Feng Bo and Rao Huiying. Interpretation of "guidelines for the prevention and treatment of chronic hepatitis B (2022 Edition)". J Clin Hepatol 2023, 39: 1553-1559.

[21] Kasuga Y, Ouda R, Watanabe M, Sun X, Kimura M, Hatakeyama S and Kobayashi KS. FBXO11 constitutes a major negative regulator of MHC class II through ubiquitin-dependent proteasomal degradation of CIITA. Proc Natl Acad Sci U S A 2023; 120: e2218955120.

[22] Thulasi Devendrakumar K, Copeland C, Adamchek C, Zhong X, Huang X, Gendron JM and Li X. Arabidopsis Tubby domain-containing F-box proteins positively regulate immunity by modulating PI4Kβ protein levels. New Phytol 2023; 240: 354-371.

[23] Yang W, Jing T, Wu C, Lu M, Yao X, Xia D and Peng D. F-box protein FBXO21 overexpression inhibits the proliferation and metastasis of clear cell renal cell carcinoma and is closely related to the CREB pathway and tumor immune cell infiltration. J Transl Med 2025; 23: 335.

[24] Zheng L, Shen J, Chen Y, Lin J, Li P, Zhao X, Ren H, Sun Y and Wang Z. FBXO43 promotes cell cycle progression in cancer cells through stabilizing SKP2. Cancer Lett 2024; 591: 216848.

[25] Deng T, Hu B, Wang X, Lin L, Zhou J, Xu Y, Yan Y, Zheng X and Zhou J. Inhibition of antiviral innate immunity by Avibirnavirus VP3 via blocking TBK1-TRAF3 complex formation and IRF3 activation. mSystems 2021; 6: e00016-21.

[26] Zeng JQ, Ruan ZL, Zhang Q, Yi XM, Chen YD, Hu MM and Li S. HTATSF1 regulates innate antiviral immune response by orchestrating TRAF3-IRF3 and TRAF6-NF-κB pathways. Cell Insight 2025; 5: 100294.

[27] Zhang Y, Cen J, Yuan G, Jia Z, Chen K, Gao W, Chen J, Adamek M, Jia Z and Zou J. DDX5 inhibits type I IFN production by promoting degradation of TBK1 and disrupting formation of

TBK1-TRAF3 complex. Cell Mol Life Sci 2023; 80: 212.
[28] Gai W, Wu M, Wu A, Jing Z, Ye Z, Jin J, Zhang Y, Zhao M, Liu G, Wang X, Yang X, Dong J, Xu Y and Zhang J. Neddylation targets and stabilizes NLRP3 to augment inflammasome-mediated colitis and mood disorder. Adv Sci (Weinh) 2026; 13: e05906.
[29] Chang PJ, Chen LW, Chen LY, Hung CH, Shih YJ and Wang SS. Effects of the NEDD8-activating enzyme inhibitor MLN4924 on lytic reactivation of kaposi's sarcoma-associated herpesvirus. J Virol 2017; 91: e00505-17.
[30] Zhang M, Qiu P, Feng Y, Yang T, Yao W, Deng Z and Wang J. Neddylation: from regulatory mechanisms to clinical implications in cancer. J Adv Res 2026; 86: 251-276.
[31] Horn-Ghetko D, Hopf LVM, Tripathi-Giesgen I, Du J, Kostrhon S, Vu DT, Beier V, Steigenberger B, Prabu JR, Stier L, Bruss EM, Mann M, Xiong Y and Schulman BA. Noncanonical assembly, neddylation and chimeric cullin-RING/RBR ubiquitylation by the 1.8 MDa CUL9 E3 ligase complex. Nat Struct Mol Biol 2024; 31: 1083-1094.
[32] Wu T, Wang Y, Shen B, Guo K, Zhu Z, Liang Y, Zeng J and Wu D. FBXO2 alleviates intervertebral disc degeneration via dual mechanisms: activating PINK1-parkin mitophagy and ubiquitinating LCN2 to suppress ferroptosis. Adv Sci (Weinh) 2025; 12: e06150.
[33] Li W, Wang Z, Liang J, Xia B, Chen R and Chen T. Role of medaka (Oryzias latipes) Foxo3 in resistance to nervous necrosis virus infection. Animals (Basel) 2024; 14: 1587.
[34] Gao D, Li S, Guo H, Liu X, Liu Z, Li L, Bao L and Dang X. A predictive model based on the FBXO family reveals the significance of cyclin f in hepatocellular carcinoma. Front Biosci (Landmark Ed) 2024; 29: 202.
[35] Xuan Z, Chen C, Sun H, Yang K, Li J, Fu M, Bai Y, Zheng Z, Zhao Y, Xu C, Liu B, Li T and Shao C. NDR1/FBXO11 promotes phosphorylation-mediated ubiquitination of β-catenin to suppress metastasis in prostate cancer. Int J Biol Sci 2024; 20: 4957-4977.
[36] Jin Y, Shenoy AK, Doernberg S, Chen H, Luo H, Shen H, Lin T, Tarrash M, Cai Q, Hu X, Fiske R, Chen T, Wu L, Mohammed KA, Rottiers V, Lee SS and Lu J. FBXO11 promotes ubiquitination of the Snail family of transcription factors in cancer progression and epidermal development. Cancer Lett 2015; 362: 70-82.
[37] Wu J, Wen T, Marzio A, Song D, Chen S, Yang C, Zhao F, Zhang B, Zhao G, Ferri A, Cheng H, Ma J, Ren H, Chen QY, Yang Y and Qin S. FBXO32-mediated degradation of PTEN promotes lung adenocarcinoma progression. Cell Death Dis 2024; 15: 282.
[38] Saha B, Olsvik H, Williams GL, Oh S, Evjen G, Sjøttem E and Mandell MA. TBK1 is ubiquitinated by TRIM5α to assemble mitophagy machinery. Cell Rep 2024; 43: 114294.
[39] Zhao X, Di Q, Chen J, Ling J, Quan J, Zhao Z, Li H, Chen S, Li X, Guo X, Wu H, Xiao Y and Chen W. The USP43/RNF2 axis negatively regulates antiviral innate immunity by promoting TBK1 ubiquitination and degradation. Cell Death Differ 2025; 32: 1806-1819.